HHS Public Access

Author manuscript

ACS Chem Neurosci. Author manuscript; available in PMC 2019 January 22.

Published in final edited form as:

ACS Chem Neurosci. 2017 November 15; 8(11): 2468–2476. doi:10.1021/acschemneuro.7b00239.

Targeting fatty-acid amide hydrolase with prodrugs for CNS-selective therapy

J. Matthew Meinig[1], **Skylar J. Ferrara**[1], **Tania Banerji**[1], **Tapasree Banerji**[1], **Hannah S. Sanford-Crane**[1], **Dennis Bourdette**[1], and **Thomas S. Scanlan**[1,*]

[1]Department of Physiology & Pharmacology, and ‡Department of Neurology, Oregon Health & Science University, 3181 SW Sam Jackson Park Road, Portland, Oregon 97239, United States.

Abstract

The blood-brain barrier (BBB) can be a substantial impediment to achieving therapeutic levels of drugs in the CNS. Certain chemical functionality such as the carboxylic acid is a general liability for BBB permeability preventing significant CNS distribution of a drug from a systemic dose. Here, we report a strategy for CNS-selective distribution of the carboxylic acid containing thyromimetic sobetirome using prodrugs targeted to fatty-acid amide hydrolase (FAAH), which is expressed in the brain. Two amide prodrugs of sobetirome were shown to be efficient substrates of FAAH with V_{max}/K_M values comparable to the natural endocannabinoid FAAH substrate anandamide. In mice, a systemic dose of sobetirome prodrug, leads to a substantial ~60-fold increase in brain distribution (K_p) of sobetirome compared to an equimolar systemic dose of the parent drug. The increased delivery of sobetirome to the brain from the prodrug was diminished by both pharmacological inhibition and genetic deletion of FAAH *in vivo*. The increased brain exposure of sobetirome arising from the prodrug corresponds to ~30-fold increased potency in brain target engagement compared to the parent drug. These results suggest that FAAH-targeted prodrugs can considerably increase drug exposure to the CNS with a concomitant decrease in systemic drug levels generating a desirable distribution profile for CNS acting drugs.

Keywords

blood-brain barrier; FAAH; thyromimetic; prodrug; sobetirome; thyroid hormone

[*]*Corresponding Author:* Mailing address: Department of Physiology & Pharmacology, Oregon Health & Science University, 3181 SW Sam Jackson Park Rd, Portland, OR 97239. scanlant@ohsu.edu.

Author Contributions

T.S.S., J.M.M., and D.B. conceived of the concept. J.M.M and S.J.F. synthesized the compounds. T.S.S., J.M.M, and S.J.F. designed the experiments. J.M.M., S.J.F., T.B., T.B., and H.S.S. carried out the experiments. T.S.S, J.M.M., S.J.F, and D.B. analyzed the results. T.S.S. and J.M.M. wrote the paper.

T.S.S. is a founder and director of NeuroVia, Inc.

Supporting Information:

Hydrolysis rates of mock vs FAAH transfected COS-7 cell homogenate, extraction efficiency of arachidonic acid verse sobetirome, HPLC traces of novel compounds, ^{1}H and ^{13}C NMR spectra

Introduction

Central nervous system (CNS) drug development suffers from regulatory approval rates below those of peripheral drugs while also having longer average development times.[1] CNS drugs must achieve therapeutic exposure levels in the CNS, and this usually involves efficient penetration of the blood-brain barrier (BBB) from a peripherally administered systemic dose. The requirement for efficient distribution to the CNS is often an impediment in drug discovery, especially in cases involving lead generation from target screening where the physicochemical requirements for BBB permeability are not taken into account. The BBB primarily consists of the endothelial cell layer surrounding the capillary network in the CNS supported by astrocytes.[2] Through the use of tight-junctions and active transport, the BBB is responsible for controlling solute permeability into and out of the CNS.[3] Problems with BBB permeability have been implicated in clinical shortcomings of drugs for therapeutic areas as diverse as cancer, HIV, and lysosomal storage disorders (LSDs), among others.[3–6] New and general strategies for improving BBB penetration and increasing CNS-specific drug exposure are needed to improve the chances for success in CNS drug development.

Our interest in CNS acting drugs is connected to the potential use of thyroid hormone agonists for treating CNS disorders that may respond favorably to thyroid hormone action. Examples include the genetic diseases MCT-8-deficiency[7] and X-linked adrenoleukodystrophy (X-ALD),[8, 9] as well as multiple sclerosis (MS), a neurological disorder involving damage to the protective myelin sheaths that envelop nerve fibers.[10] Thyroid hormone stimulates both myelin development and repair, and therapeutic agents that promote remyelination are currently lacking in the collection of drugs used for treating MS and other demyelinating diseases.[11] However, thyroid hormone (**1**, Figure 1A) is not a suitable agent for chronic treatment of demyelinating disorders due to the lack of a therapeutic index (TI) between the beneficial and the thyrotoxic effects on tissues such as heart, bone, and skeletal muscle.[12] The thyromimetic sobetirome (**2**, Figure 1A) is an attractive alternative as it displays tissue selectivity resulting in an improved TI and has progressed into clinical trials for hyperlipidemia.[13] For the goal of treating CNS disorders, sobetirome is unique among thyromimetics as it[14, 15] and close analogues[16] are the only thyromimetics known to distribute to the brain from a peripheral, systemic dose.

While sobetirome does distribute to the CNS, the fraction of the administered dose that reaches the CNS is at the lower end of the range of approved CNS drugs.[17] We have been examining strategies to increase CNS distribution of sobetirome while concomitantly decreasing peripheral exposure in an effort to create new agents with improved CNS distribution profiles. These efforts have involved the creation of ester and amide prodrugs of sobetirome that mask sobetirome in circulation and peripheral tissues, but liberate sobetirome upon hydrolysis in the CNS.[18, 19] The discovery that the best-in-class sobetirome ethanolamine ester spontaneously rearranged to the corresponding ethanolamide (**3**, Figure 1A) under physiological conditions revealed the structural similarity between this sobetirome amide derivative and anandamide (AEA, **4**, Figure 1A), one of the endogenous cannabinoid substrates for fatty acid amide hydrolase (FAAH).[19] This led to the hypothesis that FAAH was responsible for cleavage of this amide prodrug to sobetirome, suggesting

that sobetirome amides ("sobetiramides") tailored as substrates for FAAH would be a highly effective strategy for liberating sobetirome in the CNS while minimizing peripheral exposure. Here we report that FAAH-tailored sobetiramides are indeed efficient substrates for FAAH that deliver exceptionally high concentrations of sobetirome to the CNS with minimal peripheral exposure from a peripheral systemic dose.

Results

Sobetiramides as FAAH substrates

From our previous studies, the best sobetirome prodrug for generating sobetirome in the brains of mice dosed peripherally with the prodrug was an ethanolamine amide (**3**) with a structural resemblance for the endogenous FAAH substrate AEA (**4**). FAAH is a membrane bound serine hydrolase found in the brain and select peripheral tissues and intercellular signaling by AEA, oleamide (OEA, **5**, Figure 1A), and other endogenous fatty-acid amides is terminated by FAAH-catalyzed hydrolysis to fatty acids.[20, 21] In addition to endogenous cannabinoids, FAAH accepts a number of structurally diverse natural and synthetic fatty-acid amides as substrates.[22–24] This known substrate promiscuity together with a recent report that synthetic luciferin amides were viable FAAH substrates,[25] led us to synthesize FAAH-targeted amide prodrugs of sobetirome (Methods).

Two such sobetiramides, Sob-AM1 (**6**) and Sob-AM2 (**7**, Figure 1A), were tested as FAAH substrates using COS7 cell homogenate with overexpressed human FAAH similar to previous reports.[26, 27] Both Sob-AM1 and Sob-AM2 demonstrated saturation kinetics of hydrolysis (Figure 1B) with observed V_{max} values (31.4 ± 2.9 and 20.9 ± 2.5 nmol mg^{-1} min^{-1}, respectively) 4–6 fold lower than the endogenous substrate AEA (128.4 ± 2.3 nmol mg^{-1} min^{-1}). Interestingly, both prodrugs exhibited similar K_M values (1.7 ± 0.7 and 1.3 ± 0.8 μM, respectively) to that observed for AEA (1.8 ± 0.2 μM) in our experiment, which leads to V_{max}/K_M ratios that are also 4–6 fold lower than AEA (Table 1). These findings demonstrate that FAAH is capable of efficiently hydrolyzing sobetiramides *in vitro* making these compounds a novel class of synthetic FAAH substrates.

In vivo pharmacology of sobetiramides

We next evaluated whether a peripheral dose of Sob-AM1 or Sob-AM2 would deliver more sobetirome to the brain than a peripheral dose of sobetirome. Equimolar doses of the three compounds (i.p., 3.05 μmol/kg) were administered to different cohorts of mice and total brain and serum concentrations of sobetirome were quantified 1 hour post-injection. Compared to sobetirome administration, Sob-AM1 and Sob-AM2 showed average total sobetirome levels in the brain approximately 17- to 20-fold higher (Figure 2A). This increase in sobetirome in the brain from the sobetiramides was accompanied by a substantial decrease in circulating levels of sobetirome (Figure 2B). Consistent with previous reports in mice,[19] sobetirome was found to have a [brain]/[serum] ratio (K_p) of 0.03 from this single time-point experiment, whereas the sobetiramides had K_p values that were considerably larger (Figure 2C). The primary amide Sob-AM1 shows a ~20-fold increase in K_p, and the *N*-methyl amide Sob-AM2 demonstrates a remarkable 100-fold increase in K_p compared to sobetirome.

Due to its favorable CNS distribution in this 1 h assay, Sob-AM2 was further evaluated in an 8-hour time course experiment. In this experiment, mice were dosed peripherally with Sob-AM2 (i.v., 9.15 μmol/kg) and sobetirome levels in brain and serum were quantified at specific time points over the next 8 h (Figure 2D). Calculated area under the curve (AUC) values for Sob-AM2 compared with previously reported values for sobetirome and compound **3** are summarized in Table 2.[19] When comparing 8-hour exposure levels, Sob-AM2 maintains brain selectivity with K_p of 1.20 ± 0.27. This represents a 60-fold improvement over the parent drug sobetirome (0.02 ± 0.006) and a 9-fold improvement to the previous best-in-class prodrug compound **3** (0.13 ± 0.03).[19] Interestingly, Sob-AM2 exhibits a ~4-fold increased hydrolysis rate at FAAH *in vitro* compared to **3** (Table S1) suggesting the improvement in K_p could at least partially be attributed to higher cleavage rates.

We next sought to understand which regions of the brain and CNS received sobetirome exposure from a peripheral dose of Sob-AM2. Mice receiving equimolar doses (i.p., 3.05 μmol/kg) of sobetirome or Sob-AM2 were sacrificed after 1 h and brains were dissected into general anatomical regions. Concentrations of sobetirome (Figure 2E) and Sob-AM2 (Figure 2F) were quantified in the dissected regions revealing that Sob-AM2 treatment led to a general increase in sobetirome concentrations across all brain regions examined compared to the brains from animals treated with sobetirome. The largest observed changes sobetirome levels with Sob-AM2 treatment were seen in the cortex (18.9-fold), hippocampus (14.7-fold), and olfactory bulbs (14.7-fold). Increased sobetirome concentrations were also observed in the spinal cord indicating that the increased CNS penetration afforded by Sob-AM2 is not limited to the brain. In prodrug treated samples, each region contained lower levels of non-hydrolyzed Sob-AM2 compared to unmasked sobetirome and the amount of non-hydrolyzed Sob-AM2 was comparable across most regions (Figure 2F). These results demonstrate CNS-wide increases in sobetirome concentrations following peripheral doses of Sob-AM2, suggesting that prodrug cleavage is not confined to a specific region, which is consistent with the known ubiquitous expression pattern of FAAH in the CNS.[20]

In vivo validation of FAAH as prodrug target

We next endeavored to obtain evidence showing that FAAH was the hydrolase responsible for sobetiramide cleavage *in vivo*. PF-3845 is a FAAH inhibitor that readily distributes to the CNS from a peripheral dose,[28] and URB-937 is a peripherally restricted FAAH inhibitor that does not cross the BBB.[29] Mouse cohorts were injected with either vehicle or an inhibitor (i.p., 1 mg/kg) followed by a second injection of Sob-AM2 (3.05 μmol/kg). One hour later mice were sacrificed and sobetirome concentration was measured in serum, brain, and peripheral tissues. Mice that received no FAAH inhibitor (vehicle, Figure 3A–B) showed high concentration of sobetirome in the brain with substantially lower levels in the serum and peripheral tissues. Treatment with PF-3845 reduced sobetirome concentration in brain by >8-fold compared to vehicle treatment (Figure 3A). Serum and peripheral tissue levels of sobetirome were also reduced in PF-3845 treated mice. The peripherally restricted FAAH inhibitor URB-937 showed a similar pattern of decreased sobetirome in the periphery; however, brain concentrations were unaffected compared to the vehicle control (Figure 3B).

To further validate the role of FAAH in activation of sobetiramide prodrugs, *FAAH*-KO mice were employed and *in vivo* concentrations of sobetirome were measured following a peripheral dose (i.p., 3.05 μmol/kg) of Sob-AM2.[30] The *FAAH*-KO mice contained significantly lower sobetirome levels in both the brain (Figure 3C) and serum (Figure 3D) compared with wild-type mice. Additionally, the deletion of FAAH had no significant impact on the brain accumulation of sobetirome from an equimolar peripheral dose of the parent drug (Figure 3E). The combined data from FAAH-specific inhibitors and *FAAH*-KO mice demonstrate unequivocally that FAAH is the major hydrolase responsible for generating sobetirome from sobetiramide prodrugs *in vivo*.

We next asked whether the increased brain and decreased peripheral concentrations of sobetirome delivered by Sob-AM2 translated into increased brain activity with decreased peripheral activity of the parent drug. Wild-type mice were dosed peripherally (i.p.) with Sob-AM2, and expression of *Hairless* (*Hr*) and *Thrsp*, T3-responsive genes in brain and liver, respectively, was quantified.[31, 32] Both sobetirome and Sob-AM2 showed the expected dose-dependent increase in brain *Hr* and liver *Thrsp* expression 6 hours post-dose. Prodrug Sob-AM2 was approximately 30-fold more potent in inducing brain *Hr* than sobetirome (Figure 4A). Likewise, Sob-AM2 was approximately 10-fold less potent than sobetirome at liver *Thrsp* induction (Figure 4B). Taken together, these T3 target gene activation results are consistent with the regional distribution findings demonstrating that peripheral dosing of sobetiramide prodrugs leads to increased CNS and decreased peripheral levels of sobetirome via a CNS-selective prodrug cleavage mechanism involving FAAH.

Discussion

There are a few devastating CNS disorders that currently have no effective therapies and may benefit from a therapeutic strategy based on thyroid hormone action in the CNS. Allan-Herndon-Dudley Syndrome, or MCT-8-deficiency, is an X-linked inborn error that affects thyroid hormone transport from blood into certain tissues including the CNS.[7] As such, MCT-8-deficient patients are born with a hypothyroid brain and suffer the expected cognitive deficits. These patients do not benefit from thyroid hormone replacement because transport of endogenous thyroid hormone across the BBB is impaired.[7, 33] X-Linked adrenoleukodystrophy (X-ALD) is an inborn error of metabolism that leads to the accumulation of very long chain fatty acids (VLCFA) resulting from loss-of-function mutations to a peroxisomal transporter called ABCD1 necessary for VLCFA degradation.[34, 35] The elevated VLCFA levels in the CNS lead to extensive demyelination producing debilitating neurological deficits. A related peroxisomal transporter called ABCD2 that is thyroid hormone regulated can complement defective ABCD1, and both T3 and sobetirome treatment lowers elevated VLCFA levels in the periphery and CNS of *Abcd1*-deficient mice.[9] Multiple sclerosis (MS) is a more prevalent inflammatory demyelinating disease in which some clinical progress has been made developing agents that are beneficial for the inflammatory component, but there are no available therapeutics that repair the damaged myelin.[10] Because thyroid hormone plays an important role in myelin production during development and myelin repair, thyromimetics capable of penetrating the BBB such as sobetirome have been proposed for the treatment of MS.[11]

The significance of these unmet clinical needs has motivated us to investigate new strategies for increasing the CNS distribution profile of thyromimetics such as sobetirome. We have undertaken a sobetirome prodrug approach, which has led us to discover a series of amide derivatives of sobetirome, sobetiramides, containing amine functionality consistent with endogenous FAAH substrates such as AEA and OEA. Here we show that these FAAH-targeted prodrugs are indeed excellent substrates for FAAH *in vitro* and *in vivo*. Peripheral dosing of these sobetiramide prodrugs generates large concentrations of sobetirome selectively in the brain compared to peripheral organs, with a considerable 60-fold increase to the [brain]/[serum] ratio (K_p) compared to a peripheral dose of the parent drug sobetirome from an 8-hour AUC experiment. The observed K_p value of 1.2 for sobetirome delivered by Sob-AM2 represents a better CNS distribution profile than most approved CNS drugs and is an efficient example of a CNS prodrug delivery system.[17, 36, 37] This dramatic change in sobetirome distribution afforded by the FAAH-activated prodrug would be expected to confer therapeutic benefits for use as a CNS drug including the potential for using lower doses and an increased therapeutic index separating desired therapeutic effects in the CNS from peripheral effects.

The ability of FAAH to catalyze efficient hydrolysis of these non-natural substrates suggests that FAAH has wider substrate recognition with respect to the carboxylate side of the cleaved amide bond and is not limited to only fatty acids. Aromatic and biaryl ether containing carboxylic acid amides can also be FAAH substrates that are processed with high efficiency. The first reported glimpse of this property was the finding that luciferin amides were effective FAAH substrates that liberated luciferin in the CNS as an imaging tool.[25] This development led to the proposal that FAAH may be a suitable hydrolase to target for a CNS-selective prodrug,[38] an idea that is reduced to practice by the findings reported here. It will be helpful to understand the limits and generality of this approach for targeting molecules to the CNS for both research tools and therapeutic applications.

The BBB represents a formidable impediment for small molecule access to the CNS and the sobetiramide prodrugs presented here are able to penetrate this barrier with little apparent difficulty. That the carboxylic acid containing parent drug sobetirome is also BBB permeable, albeit to a considerably lesser degree, is remarkable as carboxylates are considered a significant liability for BBB permeability, and there are accordingly very few carboxylate-containing CNS drugs.[39] Should the FAAH-targeting strategy prove to be a reasonably general one in terms of FAAH substrate selectivity, perhaps more carboxylate-containing drug candidates could be considered in CNS drug discovery. If, as is the case with sobetiramides, the amide-masked carboxylate is essential for therapeutic target engagement, then this strategy will block target engagement in tissues that do not express FAAH while facilitating target engagement in FAAH-expressing tissues like the brain. This confers a desirable and potentially therapeutically beneficial distribution profile for drugs acting in the CNS.

Methods

Chemistry. General Chemistry

^{1}H and ^{13}C NMR were taken on a Bruker 400 MHz. All spectra were calibrated to the NMR solvent reference peak (chloroform-*d* or d_3-MeCN). ^{1}H coupling constants (JHH, Hz) are reported as follows: chemical shift, multiplicity (br = broad, s = singlet, d = doublet, sept= septet, m = multiplet, dd = doublet of doublets), coupling constant, and integration. High-resolution mass spectrometry (HRMS) with electrospray ionization was performed by the Bioanalytical MS Facility at Portland State University. Sobetirome and d_6-sobetirome were synthesized as previously described.[40, 41] All other reagents were purchased from Fisher, Sigma, or TCI and used as received. Analytical HPLC analysis was performed on a Varian ProStar HPLC with a Grace Altima C18, 5 μm column (4.6 × 250 mm) with a gradient (Solvent A: Water + 0.1% TFA; Solvent B: MeCN + 0.1% TFA) for B: 20–100% 0–20 minutes, 100% B 20–25min, 100%−20% B 25–26min, hold 20% B 26–30 min. Flowrate was 1 mL/min. Purity analysis of final compounds was determined to be >95% by HPLC (A_{235nm}). HPLC traces can be found in the Supplemental Information.

Synthesis of Compounds and Characterization

Sob-AM1 (6), 2-(4-(4-hydroxy-3-isopropylbenzyl)-3,5-dimethylphenoxy)acetamide—Sobetirome (250 mg, 0.76 mmol, 1 eq) is treated with MeOH (3 mL) in a sealed tube. Sulfuric acid (1 drop) is added and the reaction is sealed and then heated to 65 °C for 1 hour while stirring. The reaction is allowed to come to room temperature. TLC analysis (1:30 MeOH:DCM) shows complete conversion to the intermediate methyl ester. To the intermediate reaction mixture, ammonia (7N in MeOH, 0.76 mL, 7 eq) is added. The reaction is resealed and, again, heated to 65 °C for 1 hour. The reaction flask is allowed to return to room temperature and is added to 0.5 N NaOH (20 mL) in a separtory funnel and subsequently extracted with DCM (3 × 100 mL). The organic layers are combined, dried with Na_2SO_4, and concentrated. Purification by flash chromatography (0–6% MeOH in DCM) gave the product as a white solid (157 mg, 0.48 mmol, 63%). Purity: 95% (HPLC). ^{1}H NMR (400 MHz, Chloroform-*d*) δ 6.93 (b, 1H), 6.65–6.56 (m, 5H), 5.85 (b, 1H), 5.19 (s, 1H), 4.51 (s, 2H), 3.92 (s, 2H), 3.19 (sept, J = 6.9, 1H), 2.24 (s, 6H), 1.23 (d, J = 6.9 Hz, 6H). ^{13}C NMR (101 MHz, $CDCl_3$) δ 171.6, 155.1, 151.0, 138.9, 134.3, 131.7, 131.4, 126.1, 125.3, 115.2, 114.1, 67.0, 33.7, 27.1, 22.6, 20.5. HRMS (ESI) m/z $[M+Na^+]$ $C_{20}H_{25}NNaO_3^+$ requires 350.1727, found 350.1737

Sob-AM2 (7), 2-(4-(4-hydroxy-3-isopropylbenzyl)-3,5-dimethylphenoxy)-N-methylacetamide—The synthesis was carried out identical to **6** with sobetirome (155 mg, 0.47 mmol), but using a solution of 40% methyl amine in water (610 μL, 7.05 mmol, 15 eq) instead of ammonia. The product was isolated as a white solid (144 mg, 90%). Purity: 97% (HPLC). ^{1}H NMR (400 MHz, CD_3CN): 6.98 (br, 1 H), 6.89 (s, 1 H), 6.68 (s, 2 H), 6.62 (d, 1 H, J = 8.6 Hz), 6.54 (dd, J = 8.4, 2.4 Hz, 1 H), 4.37 (s, 2 H), 3.87 (s, 2 H), 3.16 (septet, J = 6.9 Hz, 1 H), 2.75 (d, J = 4.9 Hz, 3 H), 2.20 (s, 6 H), 1.12 (d, J = 6.9 Hz, 6 H). ^{13}C NMR (101 MHz, $CDCl_3$) δ 169.4, 155.1, 151.0, 138.9, 134.3, 131.7, 131.2, 126.1, 125.2, 115.1, 114.0, 67.2, 33.7, 27.1, 25.8, 22.6, 20.5. HRMS (ESI) m/z $[M+Na^+]$ $C_{21}H_{27}NO_3Na^+$ requires 364.1883, found m/z 364.1890.

***d_6*-Sob-AM2 (8), 2-(4-(4-hydroxy-3-(propan-2-yl-1,1,1,3,3,3-*d_6*)benzyl)-3,5-dimethylphenoxy)-*N*-methylacetamide—**The synthesis was carried out identical to **7** but using d_6-sobetirome (scaled to 28 mg, 0.08 mmol) as a starting material. The product was isolated as a white solid (24.5 mg, 84%). Purity: 97% (HPLC). ^{1}H NMR (400 MHz, Chloroform-*d*): 6.94 (d, J = 1.8 Hz, 1 H), 6.68 (br, 1 H), 6.59 (m, 4 H), 5.30 (s, 1 H), 4.51 (s, 2 H), 3.92 (s, 2 H), 3.16 (s, 1 H), 2.94 (d, *J* = 5.0, 3 H), 2.23 (s, 6 H). ^{13}C NMR (101 MHz, $CDCl_3$) δ 169.5, 155.1, 151.2, 138.9, 134.4, 131.5, 131.1, 126.1, 125.2, 115.1, 114.0, 67.2, 33.7, 26.6, 25.8, 20.5. HRMS (ESI) m/z [M+H$^+$] $C_{21}H_{22}D_6NO_3^+$: m/z 348.2240, found m/z 348.2444.

General Materials

Sobetirome and d_6-sobetirome were synthesized as previously described.[40, 41] Anandamide (AEA, #90050), PF-3845 (#13279), and URB-937 (#10674) were purchased from Cayman. Arachidonic acid was purchased from Sigma (#23401). d_{11}-Arachidonic acid was purchased from Avanti (#861810E). Fatty-acid free BSA was from Alfa Aesar (#64682). Solvents were HPLC grade from Fisher.

Plasmids

Human FAAH cDNA in a pcDNA4 backbone was kindly provided by Prof. Martin Kaczocha (Stony Brook). A C-terminal FLAG sequence was inserted by PCR using the following primers: 5'-CGCAAATGGGCGGTAGGCGTG (f_CMV) and 5'-AGACTCGAGTCACTTGTCGTCATCGTCTTTGTAGTCGGATGACTGCTTTTCAGGGGTCAT. The Kpn1/Xho1 digestion fragment was reinserted back into digested pcDNA4. The resulting pcDNA4-FAAH-FLAG construct was confirmed by sequencing (OHSU DNA Services Core).

LC-MS/MS analysis

Compound quantification was performed by LC-MS/MS as previously described[19] with modifications. Chromatography separation was performed on a Hamilton PRP-C18 column (5 μm, 2.1 × 50 mm, 100 Å) fit with a Betabasic precolumn (Thermo). The gradient mobile phase was delivered at a flow rate of 0.5 mL/min, and consisted of two solvents, A: 10 mM ammonium formate in water and B: 10 mM ammonium formate in 90% acetonitrile, 10% water. The gradient was as follows: 0–0.5 min, hold 10% B; 0.5–5.1 min, 10–98% B; 5.1–7 min, hold 98% B; 7–7.1 min, 98–10% B; 7.1–8 min, hold 10%. Sample injections were 20 μL. Either a 5500 QTRAP or 4000 QTRAP hybrid/triple quadrupole linear ion trap mass spectrometer (Applied Biosystems) were used to detect analytes with multiple-reaction-monitoring (MRM) using parent ion *m/z* and a second transition. Instrument parameters were optimized for MRM transitions by direct infusion of pure compound. Sobetirome (m/z 327.3 −> 269.3 and m/z 327.3 −> 135.0; retention time 2.88 min), d_6-sobetirome (m/z 333.0 −> 275. 2 and 333.0 −> 141.1; retention time 2.86 min), arachidonic acid (m/z 303.45 −> 259.1; retention time 5.75 min), and d_{11}-arachidonic acid (m/z 314.45 −> 270.1; retention time 5.75 min) were detected with negative mode. Sob-AM2 (m/z 342.2 −> 194 and 342.2 −> 135, retention time 4.35 min) and d_6-Sob-AM2 (m/z 348.2 −> 194.1 and 348.2 −> 141.1) were detected in positive mode using a mode switch from negative to positive.

FAAH activity in cell homogenate

The COS-7 cell line was a kind gift of Prof. Michael Cohen (OHSU). COS-7 cells (from ATCC CRL-1651) were cultured in Dulbecco's Modified Eagle's Medium supplemented with FBS (10%), penicillin (100 units/L), and streptomycin (100 μg/L). Cells (800,000/well) were seeded into 6-well plates (Falcon 353046) and left to adhere overnight. Cells were transfected with pcDNA4-FAAH-FLAG with Lipofectamine (Invitrogen) according to the manufacturer's protocol. Mock transfection controls were done with transfection reagent and no DNA. Cells were washed 4-days post transfection with cold PBS and scraped into cold TE buffer (125 mM Tris, 1 mM EDTA, pH 9) and sonicated (10 sec, 60Sonic Dismembrator, Fisher). Cell homogenates were stored at −80 °C until use. Protein concentrations were determined by a BCA assay (Pierce). Cell homogenates were diluted into reaction buffer (TE buffer + 0.1% fatty-acid free BSA). Substrates were added as 50× stocks in DMSO into 50 μL aliquots of homogenate to final concentrations between 0.5 μM and 100 μM. Homogenate protein levels (0.25 – 10 μg/mL) and time (5 – 15 min) were adjusted to maintain < 10% product conversion. Reactions were quenched with 100 μL acetonitrile and vortexed for 20 s. Samples were clarified by centrifugation (10,000 rpm, 15 min, 4 °C). The supernatant was diluted 2–50 fold depending on signal intensity into 2:1 MeCN:H_2O containing 149 or 299 nM d_{11}-arachindonic acid and 14.9 or 29.9 nM d_6-sobetirome. Samples were centrifuged again (13,200 rpm, 15 min, 4 °C). Products were quantified by LC-MS/MS with standard curves generated from mock samples. Product concentrations were corrected for differences in method extraction efficiencies between sobetirome (0.48) and arachindoic acid (0.62). Extraction efficiencies were determined by the area ratio of known quantity of labeled product spiked into a mock sample before extraction to a known quantity of unlabeled product spiked into the final solution (Figure S1). Observed rates are expressed as nmol product per mg protein homogenate per min. Hydrolysis rates from nontransfected (mock) controls were determined to be minimal and did not effect calculated values (Table S1). Kinetic parameters were determined in GraphPad Prism 7 (Michaelis-Menton fitting) and are expressed as value ± SE.

Animal studies

Experimental protocols were in compliance with the National Institutes of Health Guide for the Care and Use of Laboratory Animals and approved by the Oregon Health & Science University Institutional Animal Care & Use Committee. *FAAH*-KO mice on a C57/BL6 background were a kind gift of Prof. Benjamin Cravatt (Scripps Research Institute).[30] Wild type C57BL/6 mice, aged 8–10 weeks, were purchased from Jackson Laboratory. All mice were housed in climate-controlled rooms with a 12h/12h light-dark cycle with ad libitum access to food and water. All injections were delivered intraperitoneally (i.p.) using 1:1 saline:DMSO as a vehicle except for AUC experiments, which were delivered intravenous (i.v., tail vein). Injection volumes were standardized to 150 μL/26 g mouse. When comparing sobetirome and sobetiramides, equimolar doses were given (i.e. 3.05 μmol/kg corresponds to 1 mg/kg for sobetirome). FAAH inhibitors PF-3845 and URB-937 were injected at 1 mg/kg. Time-points for the AUC experiment were: 0.167, 0.5, 1, 2, 4, and 8 h and match previous experiments.[19] Euthanasia was carried out with CO_2 followed by cervical dislocation.

Tissue processing

Tissues were processed for LC-MS/MS analysis as previously described with slight modifications.[19] Standard curves were prepared in vehicle treated samples for each tissue to control for ion suppression in the analysis.

Serum.—Whole blood was incubated for 15 min on ice and then clarified (7,800 rpm, 15 min, 4 °C). 100 μL of serum is transferred to a new tube and stored at −80 °C until further processed. Serum samples were thawed on ice prior to treatment with 10 μL internal standards (2.99 μM d_6-sobetirome in water and/or 2.99 μM d_6-Sob-AM2 in MeCN) followed by a crash with 400 μL MeCN. Following vigorous vortexing (~20 sec), samples were centrifuged (10,000 rpm, 15 min, 4 °C). The supernatant is dried under high vacuum. Samples were treated with 400 μL 1:1 MeCN:H_2O with vigorous vortexing. When Sob-AM2 was analyzed, the resuspension step was carried out with 4:1 MeCN:H_2O. Samples are centrifuged (10,000 rpm, 15 min, 4 °C), the supernatant is transferred, and centrifuged again (13,200 rpm, 15 min, 4 °C) prior to analysis by LC-MS/MS.

Brain.—Tissue weights were determined prior to homogenization. Whole brains were treated with water (1 mL) containing 29.9 nM internal standard (d_6-sobetirome and/or d_6-Sob-AM2). Tissues were homogenized in 2 mL tubes containing 3 GoldSpec 1/8 chrome steel balls (Applied Industrial Technologies) using either a Bead Bug homogenizer or a Bead Ruptor 24. The homogenate was crashed and extracted with 4 mL MeCN and centrifuged (10,000 rpm, 15 min, 4 °C). The supernatant was transferred to glass culture tubes and dried under high vacuum. The sample residue was then treated with 400 μL 1:1 MeCN:H2O and vigorously vortexed (20 sec). When Sob-AM2 was analyzed, the resuspension step was carried out with 4:1 MeCN:H_2O. The sample is centrifuged (10,000 rpm, 15 min, 4 °C) and the resulting supernatant is transferred to an eppendorf tube. The supernatant is centrifuged again (13,200 rpm, 15 min, 4 °C) and submitted for LC-MS/MS analysis.

Liver/Kidney/Heart.—Peripheral tissues were processed identical to the brain with the following modifications. From the 1 mL liver homogenate, 0.1 g (~100 μL) of sample was further processed. The 100 μL of liver sample was extracted with 400 μL MeCN. Kidney and heart samples were homogenized in 400 μL water containing 75 nM internal standard (d_6-sobetirome). Homogenization was carried out for 120 s. Sample extraction was done with 1.2 mL MeCN.

Dissected brain regions were processed as above but with slightly different volume/weight ratios. Each dissected sample was homogenized at 2.5 μL water per 1 μg tissue. The MeCN crash and extraction was performed with 10 μL MeCN per 1 μg tissue. Following drying under vacuum, samples were reconstituted in 2.5 μL 4:1 MeCN:Water per 1 μg original tissue weight. For each treatment, each region was carried out with n=5. Due to sample loss in processing, final replicates were reduced in number for some regions: sobetirome treated hippocampus (n=4); sobetirome treated olfactory bulbs (n=4); Sob-AM2 treated olfactory bulbs (n=2). All others points were done at n=5. Data represents mean ± SEM.

Quantitative PCR

Transcripts were quantified as previously described with slight modifications and are briefly described here.[19] Mice were injected (n=3 per point) once (i.p.) with sobetirome or Sob-AM2 over a dose range. Vehicle only treated mice were used as the control. Brain and liver were collected 6 h post-injection and preserved in RNAlater (Fisher). RNA was extracted from tissue and purified using Trizol (Invitrogen) and a Pure-Link RNA Mini Kit (Invitrogen) according to the manufacturer protocol. RNA was DNase treated on the column using an RNase-Free DNase kit (Qiagen). Extracted RNA was used to synthesize cDNA using a QuantiTect Reverse Transcription kit (Qiagen). Transcripts levels were measured by qPCR using the QuantiTect SYBR green PCR kit (Qiagen). *Hairless* (*Hr*) expression (f-*Hr*: CCAAGTCTGGGCCAAGTTTG; r-*Hr*: TGTCCTTGGTCCGATTGGAA) was measure relative to *gapdh* in the brain (5' f-*Gapdh*: CCGCATCTTCTTGTGCAGTG 3'; r-*Gapdh* 5' GAGAAGGCAGCCCTGGTAAC 3'). *Thrsp* expression (f-Thrsp: 5' TGAGAACGACGCTGCTGAAA 3'; r-Thrsp: 5' TATTTCCGCGTCACCTCCTG 3') was measured relative to the 18S RNA (f-18S: 5' TTCCGATAACGAACGAGACTCT 3'; r-18S: 5' TGGCTGAACGCCACTTGTC 3') in the liver. Data was analyzed using the comparative $2^{-\Delta\Delta Ct}$ method and normalized between vehicle and the highest dose of sobetirome. Individual data points are shown as normalized fold-change ± SEM. EC_{50} values were calculated using a non-linear regression (GraphPad Prism 7 four-parameter model).

Statistical Analysis

Statistical significance was determined using one-way ANOVA (Fisher LSD) or multiple t-tests as indicated. All tests were two-tailed. Replicates in each experiment were as stated in the specific figure legend and in the corresponding methods. For animal groups, experimental numbers were informed by previous experience in the field in order to minimize total animal numbers as appropriate. Analysis was carried out in GraphPad Prism 7 and carried out without further modifications. Significance level (α) was set to <0.05. P-values are illustrated with the following symbols * P <0.05, ** P <0.01, *** P<0.001.

Supplementary Material

Refer to Web version on PubMed Central for supplementary material.

Acknowledgments

We thank Lisa Bleyle (OHSU Bioanalytical Shared Resource/Pharmacokinetics Core) for technical assistance with LC-MS/MS, Prof. Benjamin Cravatt (Scripps Research Institute) for the FAAH-KO mice, Prof. Martin Kaczocha (Stony Brook) for the pcDNA4-FAAH plasmid, and Prof. Michael Cohen (OHSU) for the COS-7 line.

Funding

This work was supported by the OHSU Laura Fund for Innovation in Multiple Sclerosis, the National Institutes of Health (DK 052798, T.S.S. & T32DK007680, support to S.J.F.), and the National Multiple Sclerosis Society (RG 5199A4/1 D.B.).

Abbreviations

BBB	blood-brain barrier

FAAH	fatty-acid amide hydrolyase
X-ALD	X-linked adrenoleukodystrophy
MS	multiple sclerosis
TI	therapeutic index
AEA	anandamide
OEA	oleamide
AUC	area-under-the-curve
KO	knock out
VLCFA	very long-chain fatty acids
i.p.	intraperitoneal
i.v.	intravenous

References

1. Pangalos MN, Schechter LE, and Hurko O (2007) Drug development for CNS disorders: strategies for balancing risk and reducing attrition, Nat. Rev. Drug Discov 6, 521–532. [PubMed: 17599084]
2. Abbott NJ, Ronnback L, and Hansson E (2006) Astrocyte-endothelial interactions at the blood-brain barrier, Nat. Rev. Neurosci 7, 41–53. [PubMed: 16371949]
3. Abbott NJ (2013) Blood–brain barrier structure and function and the challenges for CNS drug delivery, J. Inherit. Metab. Dis 36, 437–449. [PubMed: 23609350]
4. Weidle UH, Niewohner J, and Tiefenthaler G (2015) The Blood-Brain Barrier Challenge for the Treatment of Brain Cancer, Secondary Brain Metastases, and Neurological Diseases, Cancer Genom. Proteom 12, 167–177.
5. Varatharajan L, and Thomas SA (2009) The transport of anti-HIV drugs across blood–CNS interfaces: Summary of current knowledge and recommendations for further research, Antiviral Res 82, A99–A109. [PubMed: 19176219]
6. Hitchcock SA, and Pennington LD (2006) Structure−Brain Exposure Relationships, J. Med. Chem 49, 7559–7583. [PubMed: 17181137]
7. Friesema EC, Visser WE, and Visser TJ (2010) Genetics and phenomics of thyroid hormone transport by MCT8, Mol. Cell. Endocrinol 322, 107–113. [PubMed: 20083155]
8. Genin EC, Gondcaille C, Trompier D, and Savary S (2009) Induction of the adrenoleukodystrophy-related gene (ABCD2) by thyromimetics, J. Steroid Biochem. Mol. Biol 116, 37–43. [PubMed: 19406244]
9. Hartley MD, Kirkemo LL, Banerji T, and Scanlan TS (2017) A Thyroid Hormone-Based Strategy for Correcting the Biochemical Abnormality in X-Linked Adrenoleukodystrophy, Endocrinology 158, 1328–1338. [PubMed: 28200172]
10. Compston A, and Coles A (2008) Multiple sclerosis, Lancet 372, 1502–1517. [PubMed: 18970977]
11. Baxi EG, Schott JT, Fairchild AN, Kirby LA, Karani R, Uapinyoying P, Pardo-Villamizar C, Rothstein JR, Bergles DE, and Calabresi PA (2014) A selective thyroid hormone beta receptor agonist enhances human and rodent oligodendrocyte differentiation, Glia 62, 1513–1529. [PubMed: 24863526]
12. Baxter JD, and Webb P (2009) Thyroid hormone mimetics: potential applications in atherosclerosis, obesity and type 2 diabetes, Nat. Rev. Drug Discov 8, 308–320. [PubMed: 19337272]

13. Scanlan TS (2010) Sobetirome: a case history of bench-to-clinic drug discovery and development, Heart. Fail. Rev 15, 177–182. [PubMed: 19002578]

14. Trost SU, Swanson E, Gloss B, Wang-Iverson DB, Zhang H, Volodarsky T, Grover GJ, Baxter JD, Chiellini G, Scanlan TS, and Dillmann WH (2000) The Thyroid Hormone Receptor-β-Selective Agonist GC-1 Differentially Affects Plasma Lipids and Cardiac Activity, Endocrinology 141, 3057–3064. [PubMed: 10965874]

15. Takahashi N, Asano Y, Maeda K, and Watanabe N (2014) In vivo evaluation of 1-benzyl-4-aminoindole-based thyroid hormone receptor beta agonists: importance of liver selectivity in drug discovery, Biol. Pharm. Bull 37, 1103–1108. [PubMed: 24989002]

16. Devereaux J, Ferrara SJ, Banerji T, Placzek AT, and Scanlan TS (2016) Increasing Thyromimetic Potency through Halogen Substitution, ChemMedChem 11, 2459–2465. [PubMed: 27731931]

17. Doran A, Obach RS, Smith BJ, Hosea NA, Becker S, Callegari E, Chen C, Chen X, Choo E, Cianfrogna J, Cox LM, Gibbs JP, Gibbs MA, Hatch H, Hop CECA, Kasman IN, LaPerle J, Liu J, Liu X, Logman M, Maclin D, Nedza FM, Nelson F, Olson E, Rahematpura S, Raunig D, Rogers S, Schmidt K, Spracklin DK, Szewc M, Troutman M, Tseng E, Tu M, Van Deusen JW, Venkatakrishnan K, Walens G, Wang EQ, Wong D, Yasgar AS, and Zhang C (2005) The impact of P-glycoprotein on the disposition of drugs targeted for indications of the central nervous system: evaluation using the MDR1A/1B knockout mouse model, Drug Metab. Disposition 33, 165–174.

18. Placzek AT, Ferrara SJ, Hartley MD, Sanford-Crane HS, Meinig JM, and Scanlan TS (2016) Sobetirome prodrug esters with enhanced blood–brain barrier permeability, Bioorg. Med. Chem 24, 5842–5854. [PubMed: 27707627]

19. Ferrara SJ, Meinig JM, Placzek AT, Banerji T, McTigue P, Hartley MD, Sanford-Crane HS, Banerji T, Bourdette D, and Scanlan TS (2017) Ester-to-amide rearrangement of ethanolamine-derived prodrugs of sobetirome with increased blood-brain barrier penetration, Bioorg. Med. Chem 25, 2743–2753. [PubMed: 28385597]

20. Egertová M, Cravatt BF, and Elphick MR (2003) Comparative analysis of fatty acid amide hydrolase and cb1 cannabinoid receptor expression in the mouse brain: evidence of a widespread role for fatty acid amide hydrolase in regulation of endocannabinoid signaling, Neuroscience 119, 481–496. [PubMed: 12770562]

21. Cravatt BF, Giang DK, Mayfield SP, Boger DL, Lerner RA, and Gilula NB (1996) Molecular characterization of an enzyme that degrades neuromodulatory fatty-acid amides, Nature 384, 83–87. [PubMed: 8900284]

22. Boger DL, Fecik RA, Patterson JE, Miyauchi H, Patricelli MP, and Cravatt BF (2000) Fatty acid amide hydrolase substrate specificity, Bioorg. Med. Chem. Lett 10, 2613–2616. [PubMed: 11128635]

23. Lang W, Qin C, Lin S, Khanolkar AD, Goutopoulos A, Fan P, Abouzid K, Meng Z, Biegel D, and Makriyannis A (1999) Substrate Specificity and Stereoselectivity of Rat Brain Microsomal Anandamide Amidohydrolase, J. Med. Chem 42, 896–902. [PubMed: 10072686]

24. Wyffels L, Muccioli GG, De Bruyne S, Moerman L, Sambre J, Lambert DM, and De Vos F (2009) Synthesis, In Vitro and In Vivo Evaluation, and Radiolabeling of Aryl Anandamide Analogues as Candidate Radioligands for In Vivo Imaging of Fatty Acid Amide Hydrolase in the Brain, J. Med. Chem 52, 4613–4622. [PubMed: 19719235]

25. Mofford DM, Adams ST, Reddy GSKK, Reddy GR, and Miller SC (2015) Luciferin Amides Enable in Vivo Bioluminescence Detection of Endogenous Fatty Acid Amide Hydrolase Activity, J. Am. Chem. Soc 137, 8684–8687. [PubMed: 26120870]

26. Kaczocha M, Glaser ST, Chae J, Brown DA, and Deutsch DG (2010) Lipid droplets are novel sites of N-acylethanolamine inactivation by fatty acid amide hydrolase-2, J. Biol. Chem 285, 2796–2806. [PubMed: 19926788]

27. Kaczocha M, Glaser ST, and Deutsch DG (2009) Identification of intracellular carriers for the endocannabinoid anandamide, Proc. Natl. Acad. Sci. U. S. A 106, 6375–6380. [PubMed: 19307565]

28. Ahn K, Johnson DS, Mileni M, Beidler D, Long JZ, McKinney MK, Weerapana E, Sadagopan N, Liimatta M, Smith SE, Lazerwith S, Stiff C, Kamtekar S, Bhattacharya K, Zhang Y, Swaney S, Van Becelaere K, Stevens RC, and Cravatt BF (2009) Discovery and Characterization of a Highly

Selective FAAH Inhibitor that Reduces Inflammatory Pain, Chem. Biol 16, 411–420. [PubMed: 19389627]

29. Sasso O, Bertorelli R, Bandiera T, Scarpelli R, Colombano G, Armirotti A, Moreno-Sanz G, Reggiani A, and Piomelli D (2012) Peripheral FAAH inhibition causes profound antinociception and protects against indomethacin-induced gastric lesions, Pharmacol. Res 65, 553–563. [PubMed: 22420940]
30. Cravatt BF, Demarest K, Patricelli MP, Bracey MH, Giang DK, Martin BR, and Lichtman AH (2001) Supersensitivity to anandamide and enhanced endogenous cannabinoid signaling in mice lacking fatty acid amide hydrolase, Proc. Natl. Acad. Sci. U. S. A 98, 9371–9376. [PubMed: 11470906]
31. Ohba K, Leow MK, Singh BK, Sinha RA, Lesmana R, Liao XH, Ghosh S, Refetoff S, Sng JC, and Yen PM (2016) Desensitization and Incomplete Recovery of Hepatic Target Genes After Chronic Thyroid Hormone Treatment and Withdrawal in Male Adult Mice, Endocrinology 157, 1660–1672. [PubMed: 26866609]
32. Thompson CC, and Bottcher MC (1997) The product of a thyroid hormone-responsive gene interacts with thyroid hormone receptors, Proc. Natl. Acad. Sci. U. S. A 94, 8527–8532. [PubMed: 9238010]
33. Schwartz CE, and Stevenson RE (2007) The MCT8 thyroid hormone transporter and Allan–Herndon–Dudley syndrome, Best Pract. Res. Clin. Endocrinol. Metab 21, 307–321. [PubMed: 17574010]
34. Kemp S, Huffnagel IC, Linthorst GE, Wanders RJ, and Engelen M (2016) Adrenoleukodystrophy - neuroendocrine pathogenesis and redefinition of natural history, Nat. Rev. Endocrinol 12, 606–615. [PubMed: 27312864]
35. Ferrer I, Aubourg P, and Pujol A (2010) General aspects and neuropathology of X-linked adrenoleukodystrophy, Brain Pathol 20, 817–830. [PubMed: 20626743]
36. Rautio J, Laine K, Gynther M, and Savolainen J (2008) Prodrug approaches for CNS delivery, AAPS J 10, 92–102. [PubMed: 18446509]
37. Liu X, Chen C, and Smith BJ (2008) Progress in brain penetration evaluation in drug discovery and development, J. Pharmacol. Exp. Ther 325, 349–356. [PubMed: 18203948]
38. Mofford DM, and Miller SC (2015) Luciferins Behave Like Drugs, ACS Chem. Neurosci 6, 1273–1275. [PubMed: 26225810]
39. Mao F, Ni W, Xu X, Wang H, Wang J, Ji M, and Li J (2016) Chemical Structure-Related Drug-Like Criteria of Global Approved Drugs, Molecules 21, 75. [PubMed: 26771590]
40. Chiellini G, Nguyen N-H, Yoshihara HAI, and Scanlan TS (2000) Improved synthesis of the iodine-free thyromimetic GC-1, Bioorg. Med. Chem. Lett 10, 2607–2611. [PubMed: 11128634]
41. Placzek AT, and Scanlan TS (2015) New synthetic routes to thyroid hormone analogs: d6-sobetirome, 3H-sobetirome, and the antagonist NH-3, Tetrahedron 71, 5946–5951. [PubMed: 28316349]

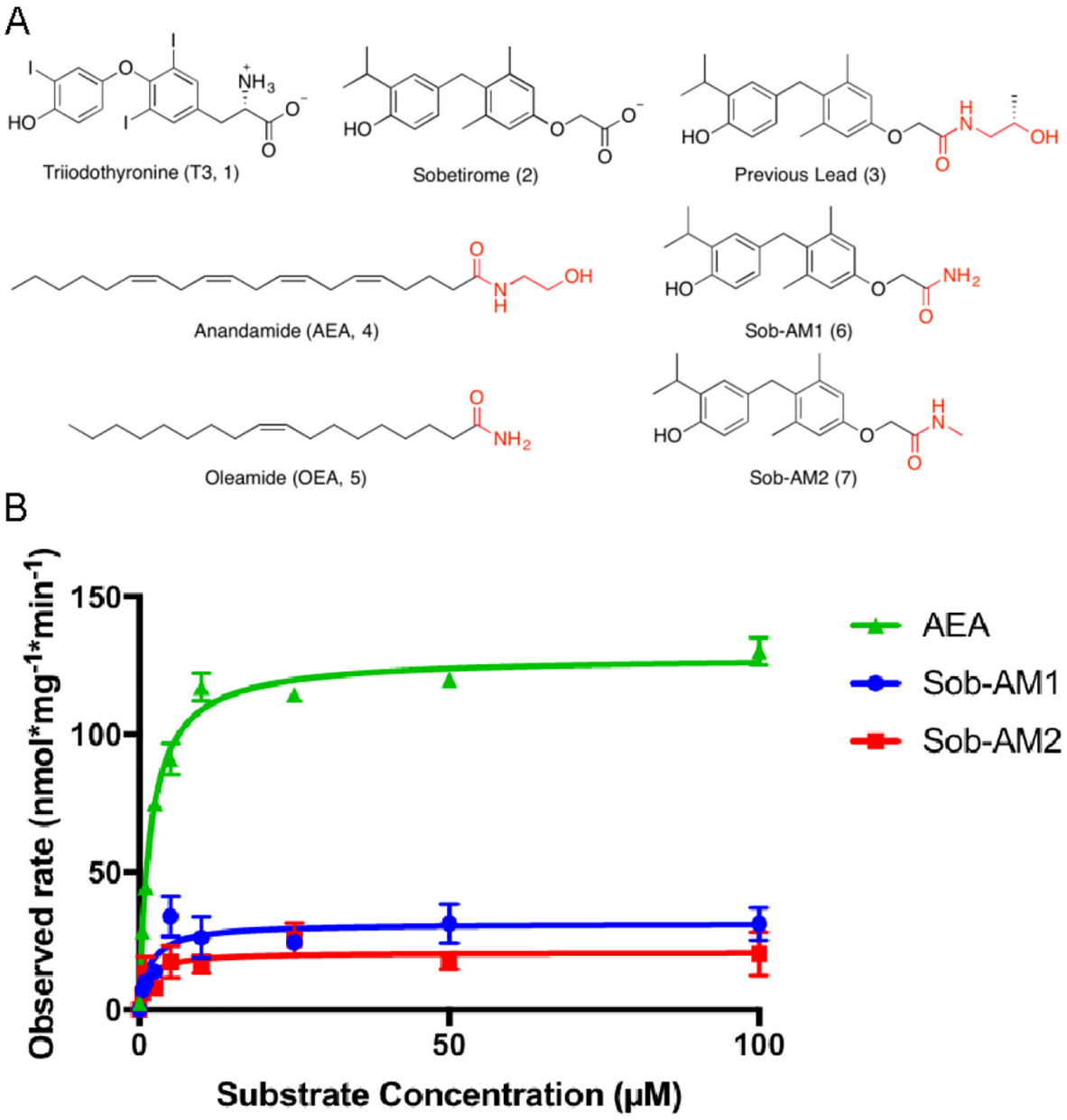

Figure 1. Sobetiramides are substrates of FAAH.

(A) Chemical structures of thyroid hormone (T3), sobetirome, two endogenous substrates of FAAH (AEA and OEA), and novel FAAH-targeted sobetirome amide (sobetiramide) prodrugs. (B) Using cell homogenate overexpressing human FAAH, Michaelis-Menten curves were produced for both Sob-AM1 and Sob-AM2 compared with the endogenous FAAH substrate AEA. Hydrolysis reactions (n=3) were monitored by quantifying product formation by LC-MS/MS. A summary of V_{max} and K_m values can be found in Table 1. For each substrate concentration, reaction time and protein levels were adjusted to maintain <10% substrate conversion. Data represent mean ± SEM

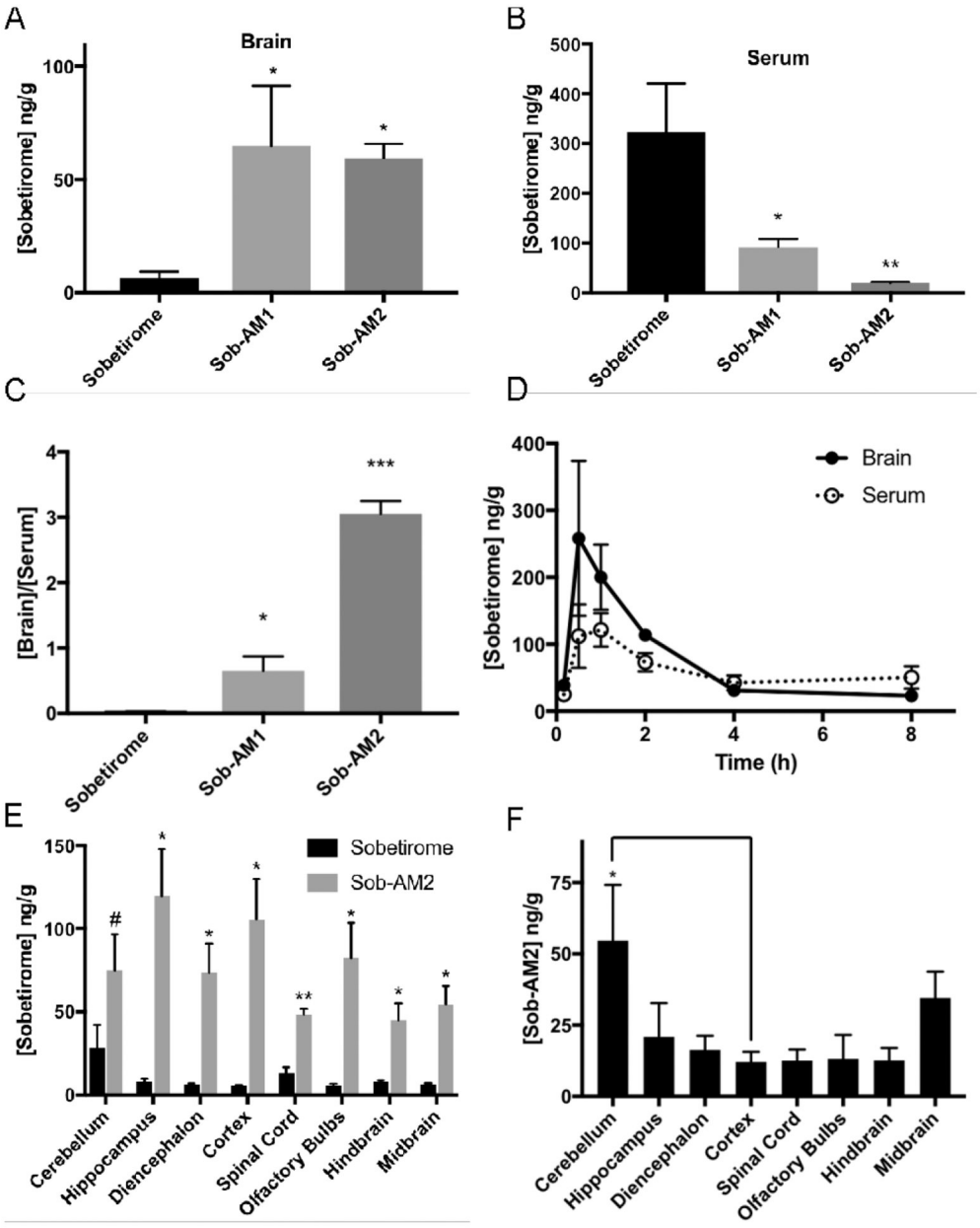

Figure 2. Sobetiramides substantially increase brain exposure while decreasing peripheral concentrations of sobetirome *in vivo*.

Mouse cohorts (n=6) were treated (i.p., 3.05 μmol/kg) with sobetirome, Sob-AM1, or Sob-AM2. After 1 h, tissues were collected and analyzed by LC-MS/MS for sobetirome levels in the (A) brain and (B) serum. (C) Brain-to-serum concentration ratios at this 1 h time point suggests significant increases in brain selective distribution of the prodrugs. Statistical analyses for A-C were done using one-way ANOVA (Fisher LSD) comparing prodrug values to sobetirome (A-C). To quantify sobetirome exposure from peripherally dosed Sob-AM over time, sobetirome levels the brain and serum (D) was measured from mouse cohorts treated at t=0 (i.v., 9.15 μmol/kg) and measured over 8 h post-dose. Each data point represents n=3. Calculated AUC values are summarized in Table 2. (E) Mice cohorts (n=3)

were treated with sobetirome or Sob-AM2 identical to A-C except brain regions were dissected and analyzed separately. Sobetirome concentrations were significantly increased in Sob-AM2 treated mice across almost all CNS regions including the cortex (18-fold) and spinal cord (3.5-fold). Statistical analyses for E were done using multiple two-tailed t-test comparing sobetirome/Sob-AM2 treatments. (F) Sob-AM2 levels were quantified in the same dissected CNS regions as (E) using LC-MS/MS monitoring the Sob-AM2 ion. Intact (non-hydrolyzed) prodrug can be observed across CNS regions at levels similar to the cortex with only the cerebellum displaying significantly elevated Sob-AM2. Statistical analysis for F was done using one-way ANOVA (Fisher LSD) comparing regions to the cortex. All data in A-F represent mean ± SEM and are expressed as a function of tissue weight. (* P= <0.05, ** P <0.01, *** P <0.001)

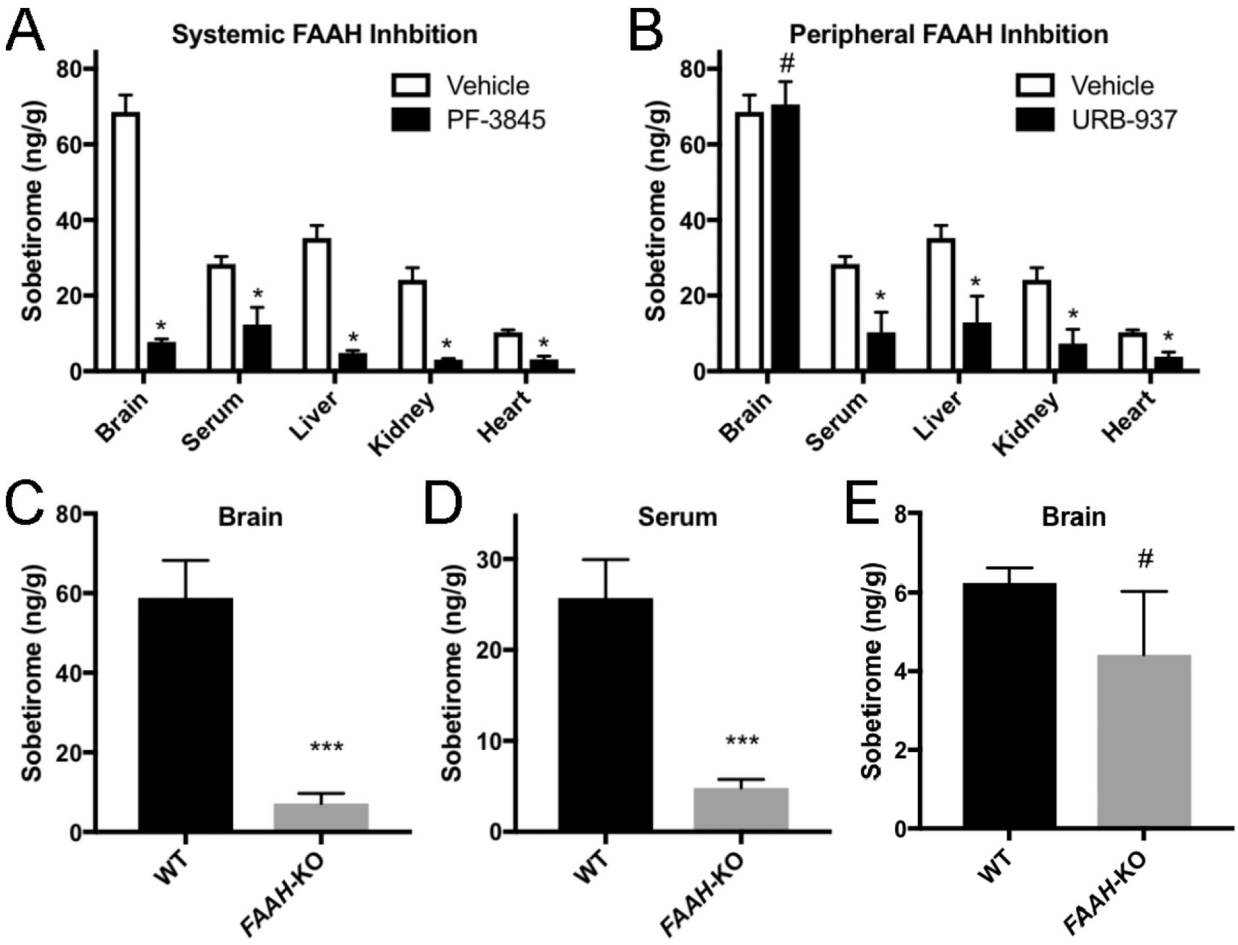

Figure 3. FAAH is the primary hydrolase responsible for sobetiramide hydrolysis in vivo.

(A & B) FAAH inhibitors significantly decrease Sob-AM2 hydrolysis in target tissues. Mouse cohorts (n=3) were treated with vehicle, PF-3845, or URB-937 (i.p., 1 mg/kg). 30 min post initial injection, mice were treated with Sob-AM2 (i.p., 3.05 μmol/kg). Tissues were collected 1 h after the second injection. (A) Consistent with its known pharmacological distribution, PF-3845 significantly reduced sobetirome levels in all tested tissues compared with vehicle. (B) Compared to the vehicle control, URB-937 reduced sobetirome levels in all tested tissues except for the brain, consistent with its inability to cross the BBB. Data for vehicle treated animals is common to (A) and (B) and is replicated for clarity. Data represent mean ± SEM and statistical analyses were performed using multiple t-test comparing inhibitor treatment to vehicle. (C-E). Wild type and *FAAH*-KO mice were treated with Sob-AM2 (i.p., 3.05 μmol/kg) and tissues were collected 1 h post-dose. Sobetirome levels analyzed by LC-MS/MS. *FAAH*-KO mice exhibited significant lowering of sobetirome in both the brain (C) and serum (D) compared to wild type animals that receiving an identical systemic dose. (E) Following a peripheral dose of the parent drug sobetirome (i.p., 3.05 μmol/kg), *FAAH*-KO mice showed no significant difference in brain sobetirome levels compared with wild type. Data represent mean ± SEM. (C) n=6; (D) and (E) n=3. Statistical analyses were performed using two-tailed Student t-tests (***P < 0.001, # P> 0.05)

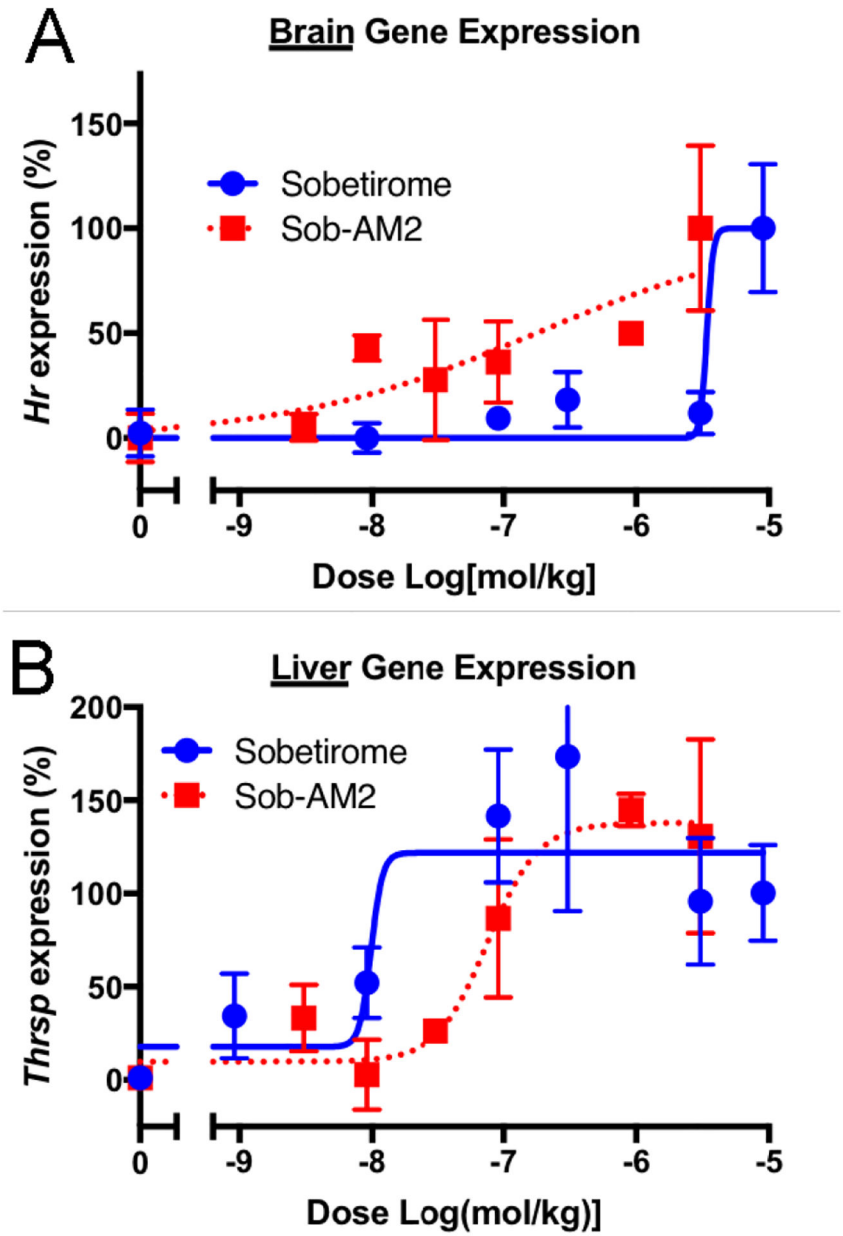

Figure 4. Sob-AM2 is more potent in the brain and less potent in the liver at TR-activation than sobetirome.

Following peripheral dosing (i.p.) of sobetirome or Sob-AM2 in wild type mice across a dose range, transcript levels of the known thyroid-responsive genes *Hr* and *Thrsp* were quantified in the brain (A) and liver (B), respectively. In the brain, Sob-AM2 (EC_{50} ~ 0.17 μmol/kg) was more potent than sobetirome (EC_{50} ~3.4 μmol/kg). This trend is reversed in the liver with *Thrsp* response (Sob-AM2 EC_{50} ~76 nmol/kg; sobetirome EC_{50} ~10 nmol/kg). Data points represent mean ± SEM and n=3.

Table 1.

A summary of Michaelis-Menten observed parameters for AEA, Sob-AM1, and Sob-AM2.

Substrate	V_{max} (nmol * mg^{-1} * min^{-1})	K_M (μM)	V_{max}/K_M
AEA	128.4 ± 2.3	1.8 ± 0.2	71.1 ± 6.3
Sob-AM1	31.4 ± 2.9	1.7 ± 0.7	18.9 ± 8.7
Sob-AM2	20.9 ± 2.5	1.3 ± 0.8	15.5 ± 9.7

Table 2.

Comparative brain and serum exposures for sobetirome, **3**, and Sob-AM2 showing systemic improvements in AUC_{brain}/AUC_{serum} (K_p).

Compound	Brain-$AUC_{0–8h}$ (ng * h * g^{-1})	Serum-$AUC_{0–8h}$ (ng * h * g^{-1})	K_p [a]
Sobetirome (**2**) [b]	9.9 ± 1.0	472.6 ± 132.4	0.02 ± 0.006
3 [b]	17.2 ± 2.3	136.5 ± 21.0	0.13 ± 0.03
Sob-AM2 (**7**) [c]	573.9 ± 82.6	479.8 ± 84.5	1.20 ± 0.27

[a] $K_p = AUC_{brain}/AUC_{serum}$

[b] Data reproduced from Ferrara, 2017 (i.p., 1.5 μmol/kg)

[c] This work (i.v., 9.15 μmol/kg)